Brazilian Journal of Medical and Biological Research (2013) 46: 235-244, http://dx.doi.org/10.1590/1414-431X20122429
ISSN 1414-431X

# Experimental model of intervertebral disc degeneration by needle puncture in Wistar rats

A.C. Issy[1], V. Castania[1], M. Castania[1], C.E.G. Salmon[2], M.H. Nogueira-Barbosa[3], E. Del Bel[1] and H.L.A. Defino[4]

[1]Departamento de Morfologia, Fisiologia e Patologia Básica, Faculdade de Odontologia de Ribeirão Preto, Universidade de São Paulo, Ribeirão Preto, SP, Brasil
[2]Departamento de Física, Faculdade de Filosofia, Ciências e Letras de Ribeirão Preto, Universidade de São Paulo, Ribeirão Preto, SP, Brasil
[3]Divisão de Radiologia, Departamento de Clínica Médica, Faculdade de Medicina de Ribeirão Preto, Universidade de São Paulo, Ribeirão Preto, SP, Brasil
[4]Departamento de Biomecânica, Medicina e Reabilitação do Sistema Locomotor, Faculdade de Medicina de Ribeirão Preto, Universidade de São Paulo, Ribeirão Preto, SP, Brasil

## Abstract

Animal models of intervertebral disc degeneration play an important role in clarifying the physiopathological mechanisms and testing novel therapeutic strategies. The objective of the present study is to describe a simple animal model of disc degeneration involving Wistar rats to be used for research studies. Disc degeneration was confirmed and classified by radiography, magnetic resonance and histological evaluation. Adult male Wistar rats were anesthetized and submitted to percutaneous disc puncture with a 20-gauge needle on levels 6-7 and 8-9 of the coccygeal vertebrae. The needle was inserted into the discs guided by fluoroscopy and its tip was positioned crossing the nucleus pulposus up to the contralateral annulus fibrosus, rotated 360° twice, and held for 30 s. To grade the severity of intervertebral disc degeneration, we measured the intervertebral disc height from radiographic images 7 and 30 days after the injury, and the signal intensity T2-weighted magnetic resonance imaging. Histological analysis was performed with hematoxylin-eosin and collagen fiber orientation using picrosirius red staining and polarized light microscopy. Imaging and histological score analyses revealed significant disc degeneration both 7 and 30 days after the lesion, without deaths or systemic complications. Interobserver histological evaluation showed significant agreement. There was a significant positive correlation between histological score and intervertebral disc height 7 and 30 days after the lesion. We conclude that the tail disc puncture method using Wistar rats is a simple, cost-effective and reproducible model for inducing disc degeneration.

Key words: Intervertebral disc degeneration; Animal models; Histology; Wistar rats

## Introduction

Degenerative disc disease (DDD) is one of the most important public health problems and one of the most common causes of low back pain (1,2). DDD is characterized by complex serial progressive morphological, biochemical and biomechanical changes of the intervertebral disc that contribute to the impairment of mechanical function and, in some cases, to the onset of discogenic low back pain (3). The causes of DDD are multifactorial and a clear understanding of the pathophysiology and pathogenesis of the condition is still lacking (4,5).

The initiation and progression of the degenerative cascade probably depend on multiple interdependent factors. It has been suggested that these factors may include reduced nutrient supply (6), hereditary factors (7), altered mechanical loading (8), age (9), up-regulated levels of proinflammatory cytokines and associated catabolic enzymes (10), and decreased diffusion of nutrients through the endplates (6). Evidently, the occurrence of one or more of these factors can promote several disc tissue changes (for a review, see Ref. 11).

Correspondence: E. Del Bel, Departamento de Morfologia, Estomatologia e Fisiologia, Faculdade de Odontologia de Ribeirão Preto, Universidade de São Paulo, 14049-904 Ribeirão Preto, SP, Brasil. E-mail: eadelbel@forp.usp.br

*Received June 18, 2012. Accepted October 16, 2012. First published online March 15, 2013.*

Animal models of intervertebral disc degeneration play an important role in clarifying pathomechanisms and testing novel therapeutic strategies for this condition (12). No ideal model for DDD currently exists, although several categories of animal models have been developed. These models can be classified as either experimentally induced (mechanical or structural models) or spontaneous, which include animals genetically altered or specially bred to develop degenerative disc disease (13,14). Many rodent disc degeneration models have been described and are advantageous for DDD because of their low cost and ease of care (15).

A recently developed needle puncture model has shown altered morphological and biochemical features similar to many of those found in human degenerative discs (4,16). In the injury model, the use of needle puncture has gained popularity mainly because of its reproducibility and the short time required to produce the desired degenerative effect (17). The rat tail disc has been proposed as a platform for the puncture model inducing disc degeneration (17-22). Rodent tail discs can be easily manipulated to induce degeneration and represent a desirable model for disc degeneration/regeneration research (20). The tail disc is accessible to intervention and does not require open exposure or tissue retraction. As a result, tail disc annular puncture involves a minimal risk of damage to surrounding structures. In addition, while human disc degeneration is a complex and multifactorial process that occurs over decades, it is clear that focal annular injury is a potential initiator of disc degeneration (23).

The needle puncture model was first described for use in the lumbar spine of rabbits (16) and, because of its advantages, was also used in rodents in a few publications, all of them using Sprague-Dawley rats (18,20-22). It is important to point out that there are differences in intervertebral discs regarding species, spinal level and age (for a review, see Ref. 12). The properties of the discs vary significantly at different locations within the spine level of the same animal, e.g., caudal and lumbar discs of the rat (24). The shape, profiles and relative sizes of the intervertebral disc and adjacent spinal tissues vary between species, with variations also occurring in the ossification centers. The variation of properties (biomechanical, morphological and cellular) between regions within the disc itself is also an important factor to consider in choosing and designing a model (12). Also, there may be variation between different colonies of the same animal strain (12). A rodent DDD model using Wistar rats, which are available in Brazil, has not been reported previously.

Thus, the objective of the present study is to describe an experimental model of DDD using Wistar rats, induced by needle puncture as a simple, less invasive and reliable method to study intervertebral disc degeneration since this method allows a complete experimental condition in the tail of the same animal. The model was validated by imaging (radiography and magnetic resonance) and histological analysis.

## Material and Methods

### Experimental animals

Sixteen Wistar rats (300-350 g) obtained from the Animal House of the Ribeirão Preto Campus, University of São Paulo, Brazil, were used. Before the experiments, the animals were housed in groups of 4 and kept at a temperature of 23 ± 1°C on a 12-h light-dark cycle. Food and drinking water were available *ad libitum*. All experiments were carried out in accordance with the Brazilian Society of Neuroscience and Behavior guidelines for animal care and all efforts were made to minimize animal suffering.

### Needle puncture technique

Animals were anesthetized with a combination of ketamine and xylazine (10:7, 100 mg/kg injected intraperitoneally). The coccygeal intervertebral spaces Co6-7, Co7-8, and Co8-9 were selected for the study. The needle puncture was performed at coccygeal intervertebral levels Co6-7 and Co8-9. The intervertebral level Co7-8 remained undisturbed as the control level. The selected coccygeal intervertebral levels (Co6-7 and Co8-9) were identified by digital palpation and confirmed by fluoroscopy. After tail skin antisepsis with alcohol iodate and using fluoroscopy, a 20-gauge needle was inserted at the level of the annulus fibrosus of Co6-7 (proximal) and Co8-9 (distal), crossing the nucleus pulposus up to the contralateral annulus fibrosus. After full penetration, the needle was rotated 360° twice and held for 30 s. The depth of needle penetration was controlled by the resistance of the contralateral annulus fibrosus.

### Magnetic resonance imaging (MRI) acquisition

MRI was performed on 9 animals 30 days after intervertebral disc puncture. Animals were anesthetized as described before so they would remain immobile throughout the entire MRI examination. Images were acquired with a 3.0 T MRI machine (Philips, Achieva, The Netherlands) using a dedicated coil for small animals. The tail was inserted into a tube containing a 0.1 M $CuSO_4$ solution to reduce the effects of susceptibility and to increase the contrast in the image. We used a 2-D spin echo-dual echo sequence with the following parameters: repetition time = 9000 ms, echo times = 16 and 80 ms, flip angle = 90, number of averages = 2, slice thickness = 0.6 mm, field of view = 40 × 40 mm, in plane resolution = 0.1 mm, 30 sagittal slices. The disc signal intensity was calculated using the T2-weighted image (echo time = 80 ms) for better visualization as an indirect measure of disc hydration since it is well known that reduction of water content is a common finding in intervertebral disc degeneration. The mean signal inten-

sity (brightness) in the control disc was set as reference for the signal intensity of the injured discs in each animal (Figure 1). Thus, the normalized intensity of the injured discs had a value between 0 and 1.

### Radiographic analysis

Radiographs of all rats were taken under anesthesia just before and after intervertebral disc puncture at 7 (n = 7) or 30 (n = 9) days. The animals were placed on a millimeter radiopaque scale to improve the identification of the intervertebral disc level (Figure 2). Radiographic images were taken with a Siemens Multix® instrument (Germany; 35 kV, 3 mA, 2.5 ms, 1 m) and were scanned and digitally stored using an image capture software program. Extreme care was taken to maintain a consistent level of anesthesia during radiography of each animal and at each time point (before and after lesion) in order to obtain a similar degree of muscle relaxation, which may affect the disc height. Therefore, based on the method proposed by Masuda et al. (4), the preoperative radiograph was always used as a baseline measurement. Using digitized radiographs, measurements including the proximal (PV) and distal (DV) vertebral body height and intervertebral disc height (DH) were analyzed using the public domain image analysis program developed by the U.S. National Institutes of Health - ImageJ (http://imagej.nih.gov/ij/) (Figure 2). Data were transported to the Excel software and the intervertebral disc height was reported as the DH index (DHI) (4). DHI was calculated by averaging the measurements obtained from the anterior (1), middle (2), and posterior (3) portions of the DH and dividing them by the average height of the adjacent vertebral body (Formula 1). Changes in the DHI of punctured discs were expressed as %DHI and normalized to the measured preoperative intervertebral disc height (Formula 2).

$$DHI = 2 * (DH1 + DH2 + DH3) / [(PV1 + PV2 + PV3) + (DV1 + DV2 + DV3)] \quad \text{(Formula 1)}$$

$$\%DHI = (DHI\ post\text{-}lesion / DHI\ pre\text{-}lesion) * 100 \quad \text{(Formula 2)}$$

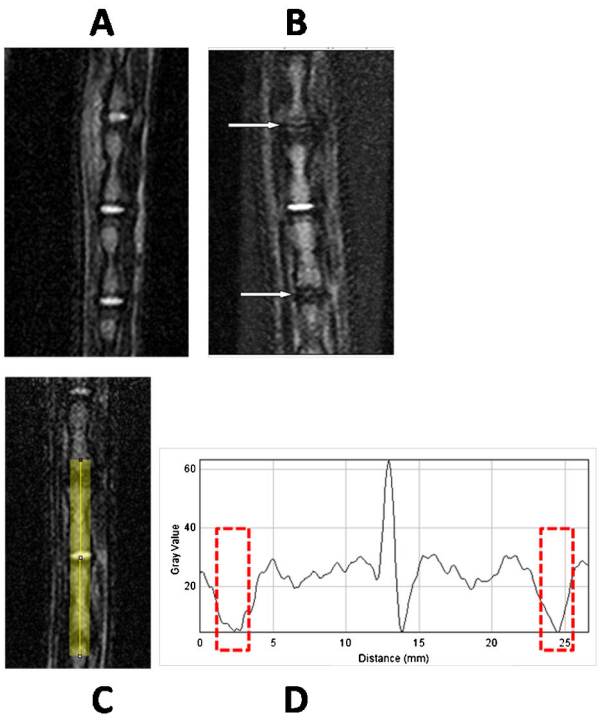


**Figure 1.** T2-weighted magnetic resonance imaging (MRI) of intervertebral discs. *A*, Normal discs before lesion. *B*, Punctured discs 30 days after lesion. The first arrow indicates the distal segment (Co8-9) and the second one the proximal segment (Co6-7). *C*, ImageJ analysis. *D*, The x-axis indicates the distance measured in millimeters and the y-axis indicates mean MRI intensity profile along the yellow line. The peak value (± 60) indicates the control segment and the depressions of the curve indicate the punctured segments marked by dashed lines on the graph. The results were normalized according to the respective control.

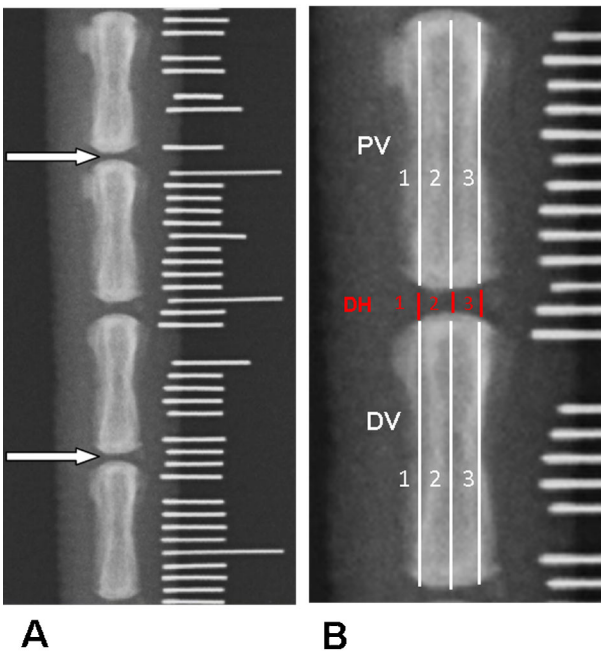


**Figure 2.** Radiographic assessment of intervertebral disc degeneration. *A*, Radiographic images were taken using a radiopaque scale with millimeter markings to recognize the intervertebral disc level of interest. Arrows indicate punctured intervertebral discs. *B*, Using digitized radiographs, measurements including the proximal (PV) and distal (DV) vertebral body height and intervertebral disc height (DH) were analyzed using the public domain image analysis program developed by the U.S. National Institutes of Health - ImageJ (http://imagej.nih.gov/ij/). 1 = anterior; 2 = middle; 3 = posterior.

### Histological analysis

Animals were sacrificed at 7 (n = 7) or 30 (n = 9) days after the tail needle puncture by excess anesthesia with ketamine/xylazine. The whole discs with the vertebrae adjacent to the punctured segments (Co6-7 and Co8-9) and non-punctured segment (Co7-8) were removed and dissected. Tissue was fixed in 4% paraformaldehyde, pH 7.4, for 24 h and decalcified in 10% ethylenediaminetetraacetic acid (EDTA) for 30 days, paraffin-embedded, and sectioned to 5-μm thickness with a microtome. The sections were stained with hematoxylin and eosin for histological score and graded in a blind fashion using the definition established by Norcross et al. (18), with some modifications (Table 1), under a light microscope (Leica®, Germany) at 10× magnification. This scale scores the disruption of the collagenous architecture and cellularity of the nucleus but not the vascular changes. The slides were graded based on the histological appearance of the characteristics of the nucleus pulposus and annulus fibrosus. The qualitative analysis of collagen fiber organization was performed using picrosirius red staining and polarized light.

### Picrosirius red

Sagittal sections of intervertebral discs and adjacent vertebral body segments were stained with picrosirius red to visualize changes in collagen organization/orientation. The slides were initially deparaffinized in xylene (3 changes - 10 min), followed by two ethanol washes - first absolute ethanol (3 changes - 3 min) and next 95% ethanol (v/v; 3 min), and washed rapidly in water. Tissue sections were stained with picrosirius (0.5 g Sirius red and 500 mL saturated picric acid) for 1 h and were again washed rapidly in water and 95% ethanol since Sirius red is soluble in water. Tissue sections were then washed in several changes of absolute ethanol (3 changes - 3 min) cleared in xylene (3 changes - 3 min) and mounted.

### Reliability of images and histological analyses

To assess the interobserver reliability of the analyses, 2 authors independently performed histological rating. The degree of interobserver agreement regarding the histological analyses was determined using the Cohen kappa coefficient.

### Statistical analyses

The normalized intensity values from MRI were analyzed by the paired *t*-test. Intervertebral disc height and histological score were analyzed by univariate analysis of variance with condition (control or lesion segments) as between-subject comparison. All tests were followed by the Duncan test for multiple comparisons ($P < 0.05$). Histological score and intervertebral disc height data were tested by Pearson's correlation analysis.

## Results

### MRI

The T2-weighted images retrieved from serial imaging

**Table 1.** Histological grading scale criteria based on Norcross et al. (18).

| Histological grading scale |
|---|
| Nucleus pulposus (NP) |
| 5. Large, bulging central cavity with abundant NP material; >2/3 intervertebral disk (IVD) height; smooth borders with minimal disruption |
| 4. Slightly reduced central cavity size with some NP material present; >1/3 IVD height and <2/3 IVD height; minimal border disruption may be present |
| 3. Markedly reduced and disrupted cavity with minimal NP material and compartmentalization; total cavity >1/3 IVD height and <2/3 IVD height |
| 2. Severe disruption of NP with minimal cavity; total cavity <1/3 IVD height but >0; consists only of a few small pockets lined by NP-like cells |
| 1. Complete obliteration of cavity with no NP-lined pockets |
| Annulus fibrosus (AF) |
| 5. Discrete, well-opposed lamellae bulging outward with no infolding; minimal preparation defect with ''simple radial clefting'' |
| 4. Discrete lamellae, less well-opposed; minimal infolding may be present; fibers remain well-organized, but with ''complex radial clefting'' |
| 3. Moderate to severe infolding of discrete, relatively well-opposed lamellae; moderate fragmentation of lamellae; AF fibers remain well organized |
| 2. Severe infolding and distortion of poorly opposed lamellae; severe fragmentation of lamellae; small regions of disorganized fibrous material replacing central lamellae |
| 1. Severe infolding, distortion, and fragmentation of lamellae; extensive amount of disorganized fibrous material replacing central lamellae |

This scale mainly scores the disruption of nucleus pulposus central cavity and cellularity and collagen fiber orientation of annulus fibrosus. Simple radial clefting = the presence of radial gaps between AF lamellae with minimal fragmentation; complex radial clefting = the presence of radial, transverse, and/or oblique gaps in the lamellae with significant fragmentation.

studies of the coccygeal disc showed degeneration of the disc 30 days after needle puncture. A decrease of signal intensity was observed in punctured discs and the control discs did not reveal loss of the signal. The control disc remained consistent over the 30-day period of evaluation. Punctured discs showed a significant decrease of the MRI signal compared to control discs (Co8-9: $t_8 = -4.75$; $P < 0.001$ and Co6-7: $t_8 = 8.49$; $P < 0.001$) (paired *t*-test, $P < 0.05$) (Figure 3) 30 days after the lesion. We did not detect any difference in MRI signal between punctured discs (Co8-9 and Co6-7).

### Radiographic assessment

Radiographic assessment of the disc height was performed considering the DHI, that was calculated by averaging measures before and after disc needle puncture. The control discs showed no significant differences among time points. Punctured discs showed a significant decrease in intervertebral DHI compared to control discs [$F(5,48) = 6.83$; $P = 0.001$] 7 and 30 days after tail needle puncture (univariate analysis of variance followed by the *post hoc* Duncan test, $P < 0.05$; Table 2). The effect of time after needle puncture on DHI was not statistically significant. No significant difference in intervertebral disc height was observed between punctured discs (Co8-9 and Co6-7), or between 7 and 30 days after lesion.

### Histological score

Histological sections of the nucleus pulposus and annulus fibrosus showed a range of morphological changes after needle puncture. The nucleus pulposus and annulus fibrosus of punctured discs showed significant alterations compared to control discs 7 and 30 days after lesion [$F(11,180) = 19.50$; $P = 0.001$] by univariate analysis of variance followed by the *post hoc* Duncan test, $P < 0.05$ (Figures 4 and 5). No significant difference in histological score was observed between punctured discs (Co8-9 and Co6-7), or between 7 and 30 days after lesion. The only difference found was in the annulus fibrosus score between 7 and 30 days after lesion. Since we detected a significant degree of histological interobserver agreement determined by the Cohen kappa coefficient, the data are reported as the average of observers 1 and 2 (Figure 4). Collagen fiber orientation was assessed using picrosirius red staining and polarized microscopy and is shown in Figure 6.

### Correlations between techniques

Pearson's correlation ($P < 0.05$) analyses revealed a significant positive correlation between histological score

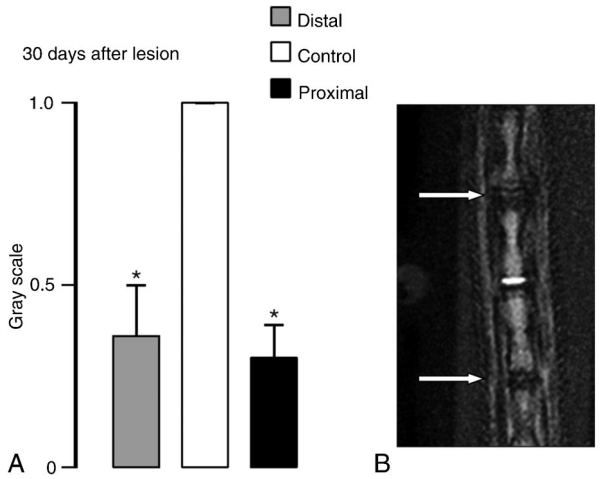


**Figure 3.** Normalized magnetic resonance imaging (MRI) signal evaluated 30 days after lesion in the three discs. *A*, Punctured distal (Co8-9) and proximal (Co6-7) discs showed a significant decrease of MRI signal compared to control. We did not detect any difference in MRI signal between proximal and distal segments. *P < 0.05 compared to control (paired *t*-test). *B*, MRI T2-weighted signal of punctured discs Co8-9 (top arrow) and Co6-7 (bottom arrow) and the intermediate disc as a control (Co7-8).

**Table 2.** Percentage of disc height index (%DHI).

| Disc segment | Time after lesion | |
|---|---|---|
| | 7 days | 30 days |
| Co(6-7) | 71.5 ± 6.70* | 60.0 ± 6.70* |
| Co(7-8) | 98.6 ± 5.02 | 93.5 ± 2.30 |
| Co(8-9) | 76.2 ± 10.65* | 62.8 ± 7.50* |

Punctured discs (Co6-7 and Co8-9) showed a significant decrease of %DHI 7 and 30 days after lesion. *P < 0.05 compared to control disc (Co7-8) (univariate analysis of variance followed by the *post hoc* Duncan test). Based on previous published research (31).

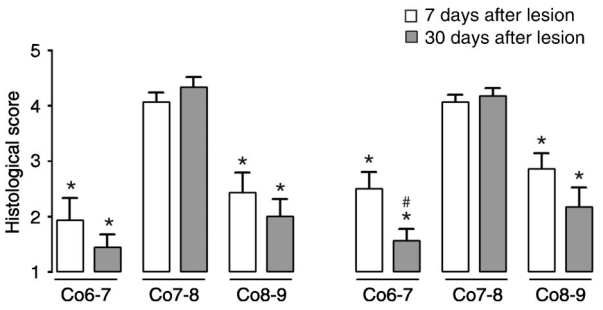


**Figure 4.** Histological analysis of the nucleus pulposus (left) and annulus fibrosus (right) 7 and 30 days after lesion. Punctured proximal and distal discs showed a significant decrease of histological score compared to control (Co7-8). There was no difference between proximal and distal discs. The Cohen kappa coefficient showed a significant degree of histological interobserver agreement. *P < 0.05 compared to control; #P < 0.05 compared to 7 days (univariate analysis of variance followed by the *post hoc* Duncan test).

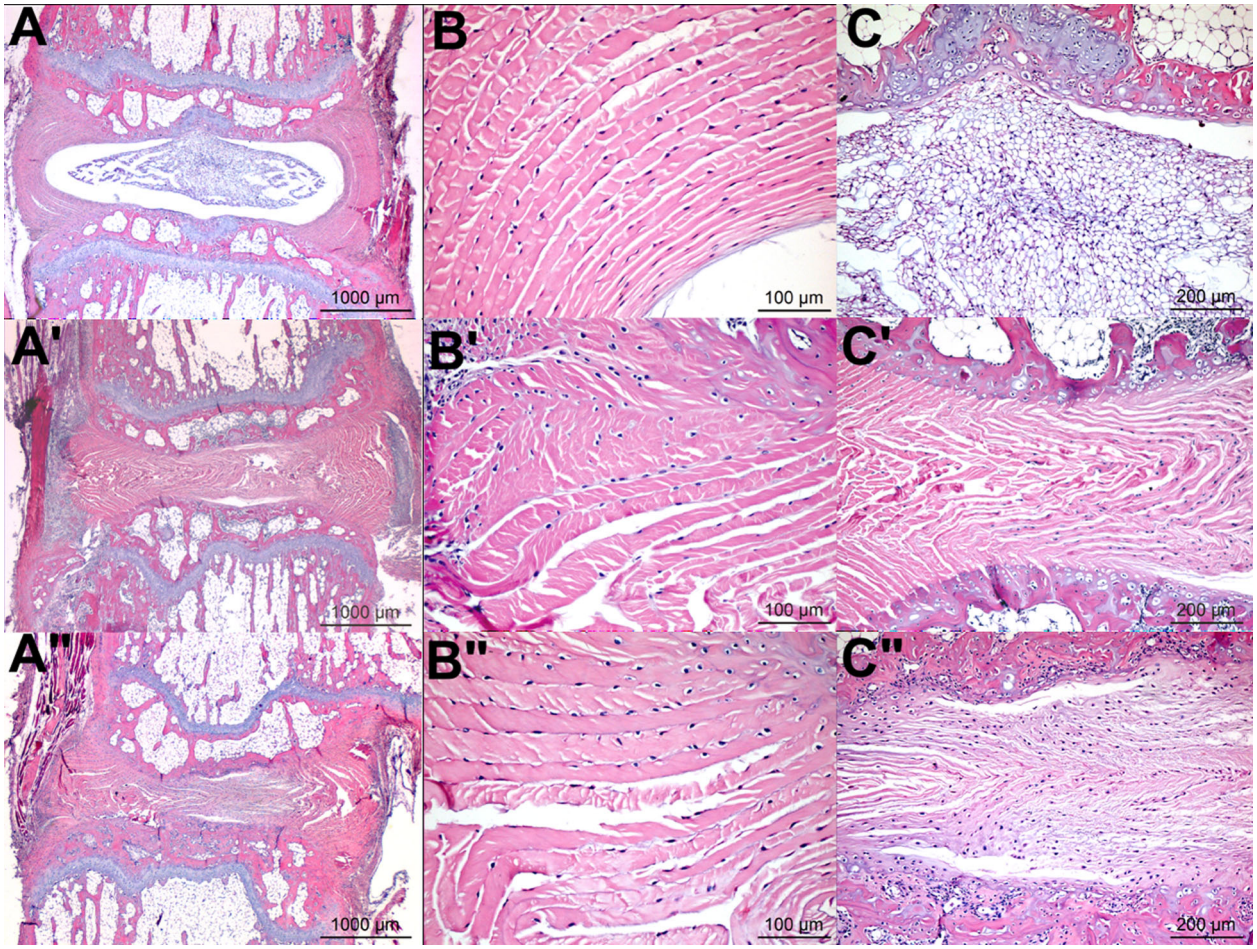


**Figure 5.** Representative sections stained with hematoxylin and eosin of intact control and punctured discs 7 or 30 days post-lesion. *A*, Intact control showing an unbroken annulus fibrosus with its border clearly defined and the nucleus pulposus comprising a significant disc area in the sagittal sections. *B*, Annulus fibrosus of an intact disc with well-opposed lamellae. *C*, Nucleus pulposus of a large intact disc with abundant material. Punctured disc 7 (*A′*) or 30 days (*A″*) after lesion showing poorly opposed lamellae and complete obliteration of the nucleus pulposus cavity. Annulus fibrosus of punctured discs with severe lamellar disorganization/fragmentation 7 (*B′*) or 30 days (*B″*) after lesion. Nucleus pulposus cavity of punctured discs without true nucleus pulposus cells replaced with fibrous material 7 (*C′*) or 30 days (*C″*) after lesion.

and intervertebral disc height 7 and 30 days after lesion in both regions (nucleus pulposus and annulus fibrosus). Linear regression curves are presented in Figure 7. We did not calculate the correlation between histological score and MRI because we tested only the latest time (30 days after lesion) by MRI.

## Discussion

Percutaneous needle puncture induces degenerative signs similar to those of human discs (16,18,20-22). Needle puncture of the caudal discs of Wistar rats induced early and clear degeneration very similar to that previously reported for rabbits or Sprague-Dawley rats (16,20-22). The described model is simple and economic and seems to be appropriate for investigating the pathogenesis of intervertebral disc degeneration. Image and histological outcome measures validated the model presented here and may strongly predict the severity of disc degeneration.

The main features observed included disc space narrowing, decreased disc height, water content reduction, and histological disorganization. Among classical histological alterations, we detected changes ranging from discrete disruption of the nucleus pulposus and a small decrease of its cavity to its complete obliteration and absence of nucleus pulposus cells. Similarly, we were able to measure different degrees of lamellar disorganiza-


**Figure 6.** Collagen fiber orientation was assessed using picrosirius red staining and examined under polarized light. The upper panel shows a control intervertebral disc (*A*) and the same disc viewed by polarizing microscopy (*A'*). The lower panel shows the same condition with a lesioned disc (*B* and *B'*). Collagen type I fibers are shown in green in the annulus fibrosus, and collagen type II fibers are shown in red. Proliferation of collagen type I fibers was detected in the nucleus pulposus space of a lesioned disc.

tion of the annulus fibrosus. These results are similar to those first obtained with Sprague Dawley rats (20-22).

We already know that in experimental models the severity of intervertebral disc degeneration is directly correlated to the needle gauge used. A larger diameter needle consistently resulted in degeneration (16,20,21). The severity of disc degeneration could be reasonably calculated by the selection of needle gauge. Small diameter needles, for example more than 30 gauge, could be used to inject gene therapy agents or several other biological agents for disc manipulation. According to our results, the 20-gauge needle was able to induce important disc degeneration 7 days after lesion, and these results were not different 30 days post-lesion. Therefore, our model did not reveal any spontaneous regeneration and suggests a stable injury. In a recent publication, Zhang et al. (22) reported that 21-gauge needle puncture into the rat tail disc induces a rapid and progressive disc degeneration process without spontaneous recovery.

Comparing our results for 7 and 30 days after injury, a tendency to progressive disc degeneration was detected in DHI (Table 2) and in the histological score (Figure 4). This progressive injury is a relevant representation of disc degeneration in humans and is suitable for evaluating the effectiveness of new treatments (4). Also, the significant correlations between %DHI values and histological results (Figure 7) confirm that DHI can be used as a good indicator of the injury (4).

Additionally, we did not find any difference in MRI signal between proximal and distal segments (Figure 3). The same finding was repeated in radiographic (Table 2) and histological data (Figure 4). This independence between the injury and different segments of the caudal level suggest that in this model several conditions could be tested in the same tail. Indeed, we conducted another cohort of experiments (data not shown here) using adjacent coccygeal intervertebral levels to promote a complete experimental condition in order to test the effect of an innocuous substance (as control) or the drug of interest either in a lesioned or intact disc with success (Figure 8).

The annulus puncture model for inducing disc degeneration was initially used in the lumbar spine of rabbits (16). Rodent tail disc degeneration was later used considering its easy manipulation since it does not require a surgical procedure (20). Additionally, the tail disc degeneration model induced by needle puncture is a simplified low-cost procedure. To our knowledge, the use of Wistar rats as an animal model for disc degeneration has not been reported before. Basically, animal models of

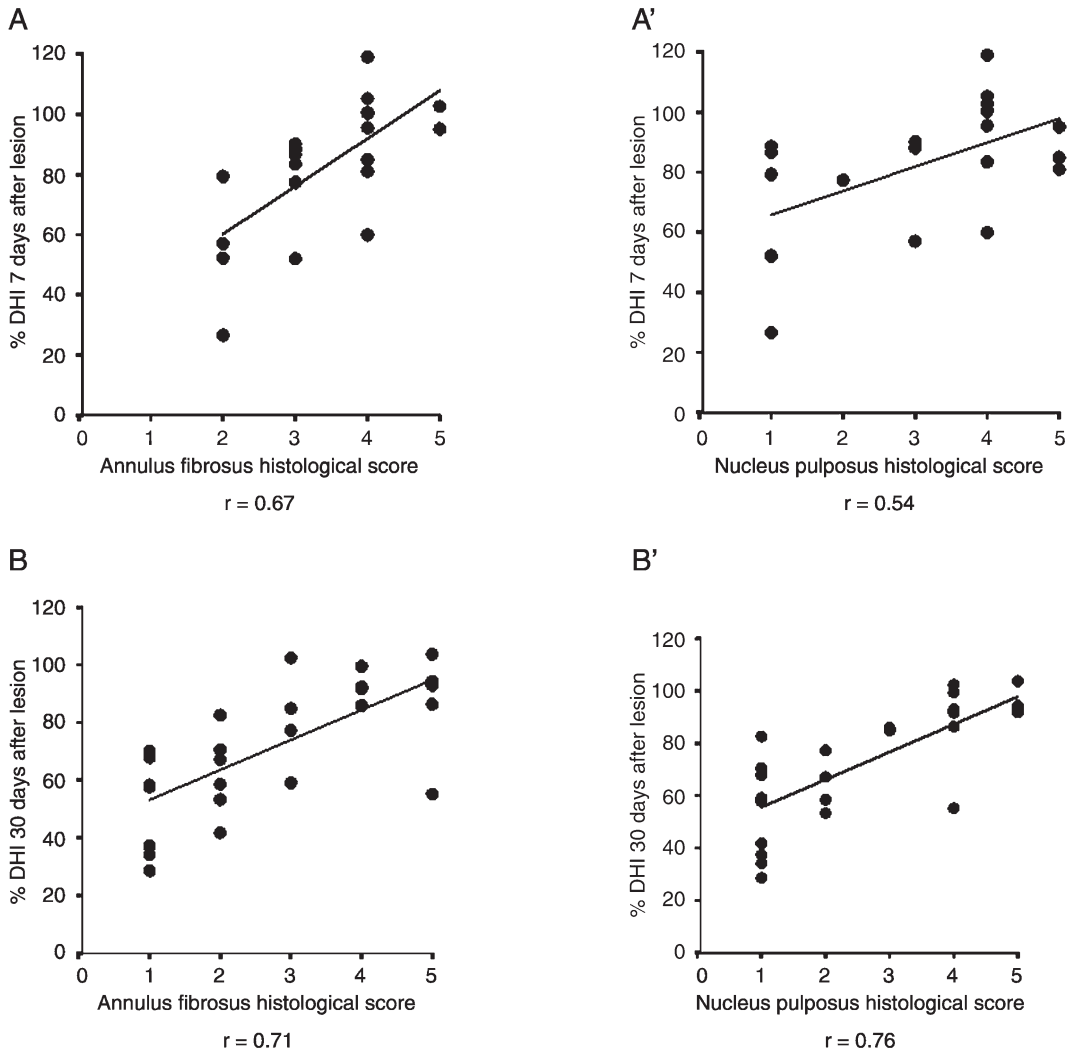


**Figure 7.** The graphs represent the linear regression of data obtained by radiographic and histological analysis of the nucleus pulposus and annulus fibrosus at 7 and 30 days after surgery. Pearson's correlation coefficients obtained were: 7 days post-injury - annulus fibrosus: $r = 0.67$, $P < 0.01$ (*A*) and nucleus pulposus: $r = 0.54$, $P < 0.05$ (*A'*); 30 days after injury - annulus fibrosus: $r = 0.71$, $P < 0.01$ (*B*) and nucleus pulposus: $r = 0.76$, $P < 0.01$ (*B'*). DHI = disc height index.

disc degeneration must be ethical, uncomplicated, reproducible, and controllable, of low cost, effective and clinically relevant to the human situation. According to our results, the use of Wistar rats fulfilled most of the expected requirements. Therefore, we found a significant degree of agreement in histological interobserver evaluation and a significant positive correlation between histological score and intervertebral disc height 7 and 30 days after injury, characteristics that validate the tools used in the current model.

Acute herniation and subsequent nucleus depressurization are considered to be the basic mechanism initiated by the degenerative cascade after annulus fibrosus puncture (13). The disruption of the annulus fibrosus in several animals and also in humans has induced disc degeneration (25-27). In fact, in the tail puncture model, the rate of degeneration is positively related to the depth of needle puncture, i.e., half or full penetration of the annulus fibrosus (20).

As mentioned before, the tail model became attractive because its discs are accessible to interventions, with minimal risk of damage to surrounding structures, and minimal interference with normal physiological function (12). However, the limitations and drawbacks of the experimental model of rat tail puncture should be recognized. Although this model has the advantage of being inexpensive compared to larger animals, the cell biology and biochemistry of the rat nucleus pulposus do not resemble those of mature humans (28). The intervertebral discs of small animals consist predominantly of

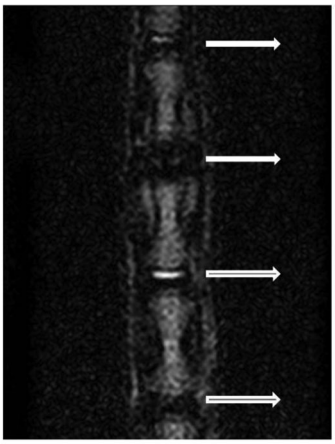


**Figure 8.** Hypothetical experimental design at adjacent coccygeal intervertebral levels. This technique allows testing the effect of an innocuous substance or vehicle as control (ex., saline) or the drug of interest both in an injured and uninjured disc.

notochordal cells embedded in gelatinous material, whereas human vertebral discs consist mostly of chondrocyte-like cells embedded in a fibrocartilaginous matrix. In humans, intervertebral disc notochordal cells are present in a limited number until the age of 12 years, while in small animals these cells remain and are not replaced. Also, this model has the disadvantage that rodents' tail discs are clearly different from lumbar discs in terms of biomechanics and composition. Furthermore, it is important to consider that the tail disc has been suspected to have lesser loading and different anatomy and dimensions (for a review, see Ref. 12).

Nevertheless, we should consider that this tail puncture model permits simple, efficient, inexpensive, and numerous experimental evaluations to test different treatment modalities (18). Significantly, this model also raises the intriguing question of whether the attempted therapeutic injection in human discs can paradoxically lead to degeneration because of the needle puncture (29). Clinical studies have already found that actual needle puncture into the disc may have contributed to the progression of disc degeneration (27,30).

Although the pathological changes involved in DDD have been well described (3,7,9,10), further studies are needed to elucidate the nature of these events, the mechanism of pain in DDD and possible intervention therapies. In conclusion, we believe that the Wistar rat tail puncture model is an attractive tool to be used in further studies to better understand DDD and explore potential treatments for this condition.

## Acknowledgments

The authors are grateful to Célia Aparecida da Silva for technical support, to Dr. João Walter de Souza da Silveira for help with the hematoxylin-eosin photographs of this study, to Joost J.A. de Jong for his expert assistance with the radiographic and MRI analysis and CNPq, FAPESP and NAPNA-USP. Research supported by CAPES/PNPD.

## References

1. Sive JI, Baird P, Jeziorsk M, Watkins A, Hoyland JA, Freemont AJ. Expression of chondrocyte markers by cells of normal and degenerate intervertebral discs. *Mol Pathol* 2002; 55: 91-97, doi: 10.1136/mp.55.2.91.
2. Richardson SM, Mobasheri A, Freemont AJ, Hoyland JA. Intervertebral disc biology, degeneration and novel tissue engineering and regenerative medicine therapies. *Histol Histopathol* 2007; 22: 1033-1041.
3. Urban JP, Roberts S. Degeneration of the intervertebral disc. *Arthritis Res Ther* 2003; 5: 120-130, doi: 10.1186/ar629.
4. Masuda K, Aota Y, Muehleman C, Imai Y, Okuma M, Thonar EJ, et al. A novel rabbit model of mild, reproducible disc degeneration by an anulus needle puncture: correlation between the degree of disc injury and radiological and histological appearances of disc degeneration. *Spine* 2005; 30: 5-14.
5. Podichetty VK. The aging spine: the role of inflammatory mediators in intervertebral disc degeneration. *Cell Mol Biol* 2007; 53: 4-18.
6. Urban JP, Smith S, Fairbank JC. Nutrition of the intervertebral disc. *Spine* 2004; 29: 2700-2709, doi: 10.1097/01.brs.0000146499.97948.52.
7. Battie MC, Videman T. Lumbar disc degeneration: epidemiology and genetics. *J Bone Joint Surg Am* 2006; 88 (Suppl 2): 3-9, doi: 10.2106/JBJS.E.01313.
8. Stokes IA, Iatridis JC. Mechanical conditions that accelerate intervertebral disc degeneration: overload versus immobilization. *Spine* 2004; 29: 2724-2732, doi: 10.1097/01.brs.0000146049.52152.da.
9. Zhao CQ, Wang LM, Jiang LS, Dai LY. The cell biology of intervertebral disc aging and degeneration. *Ageing Res Rev* 2007; 6: 247-261, doi: 10.1016/j.arr.2007.08.001.
10. Le Maitre CL, Freemont AJ, Hoyland JA. The role of interleukin-1 in the pathogenesis of human intervertebral disc degeneration. *Arthritis Res Ther* 2005; 7: R732-R745, doi: 10.1186/ar1732.
11. Freemont AJ. The cellular pathobiology of the degenerate intervertebral disc and discogenic back pain. *Rheumatology* 2009; 48: 5-10, doi: 10.1093/rheumatology/ken396.
12. Alini M, Eisenstein SM, Ito K, Little C, Kettler AA, Masuda K, et al. Are animal models useful for studying human disc disorders/degeneration? *Eur Spine J* 2008; 17: 2-19, doi: 10.1007/s00586-007-0414-y.
13. Lotz JC. Animal models of intervertebral disc degeneration: lessons learned. *Spine* 2004; 29: 2742-2750, doi: 10.1097/01.brs.0000146498.04628.f9.
14. Singh K, Masuda K, An HS. Animal models for human disc

degeneration. *Spine J* 2005; 5: 267S-279S, doi: 10.1016/j.spinee.2005.02.016.
15. Rousseau MA, Ulrich JA, Bass EC, Rodriguez AG, Liu JJ, Lotz JC. Stab incision for inducing intervertebral disc degeneration in the rat. *Spine* 2007; 32: 17-24, doi: 10.1097/01.brs.0000251013.07656.45.
16. Sobajima S, Kompel JF, Kim JS, Wallach CJ, Robertson DD, Vogt MT, et al. A slowly progressive and reproducible animal model of intervertebral disc degeneration characterized by MRI, X-ray, and histology. *Spine* 2005; 30: 15-24.
17. Keorochana G, Johnson JS, Taghavi CE, Liao JC, Lee KB, Yoo JH, et al. The effect of needle size inducing degeneration in the rat caudal disc: evaluation using radiograph, magnetic resonance imaging, histology, and immunohistochemistry. *Spine J* 2010; 10: 1014-1023, doi: 10.1016/j.spinee.2010.08.013.
18. Norcross JP, Lester GE, Weinhold P, Dahners LE. An *in vivo* model of degenerative disc disease. *J Orthop Res* 2003; 21: 183-188, doi: 10.1016/S0736-0266(02)00098-0.
19. Ulrich JA, Liebenberg EC, Thuillier DU, Lotz JC. ISSLS prize winner: repeated disc injury causes persistent inflammation. *Spine* 2007; 32: 2812-2819, doi: 10.1097/BRS.0b013e31815b9850.
20. Han B, Zhu K, Li FC, Xiao YX, Feng J, Shi ZL, et al. A simple disc degeneration model induced by percutaneous needle puncture in the rat tail. *Spine* 2008; 33: 1925-1934, doi: 10.1097/BRS.0b013e31817c64a9.
21. Zhang H, La Marca F, Hollister SJ, Goldstein SA, Lin CY. Developing consistently reproducible intervertebral disc degeneration at rat caudal spine by using needle puncture. *J Neurosurg Spine* 2009; 10: 522-530, doi: 10.3171/2009.2.SPINE08925.
22. Zhang H, Yang S, Wang L, Park P, La Marca F, Hollister SJ, et al. Time course investigation of intervertebral disc degeneration produced by needle-stab injury of the rat caudal spine: laboratory investigation. *J Neurosurg Spine* 2011; 15: 404-413, doi: 10.3171/2011.5.SPINE10811.
23. Iatridis JC, Michalek AJ, Purmessur D, Korecki CL. Localized intervertebral disc injury leads to organ level changes in structure, cellularity, and biosynthesis. *Cell Mol Bioeng* 2009; 2: 437-447, doi: 10.1007/s12195-009-0072-8.
24. Elliott DM, Sarver JJ. Young investigator award winner: validation of the mouse and rat disc as mechanical models of the human lumbar disc. *Spine* 2004; 29: 713-722, doi: 10.1097/01.BRS.0000116982.19331.EA.
25. Moore RJ, Latham JM, Vernon-Roberts B, Fraser RD. Does plate fixation prevent disc degeneration after a lateral anulus tear? *Spine* 1994; 19: 2787-2790, doi: 10.1097/00007632-199412150-00010.
26. Olsewski JM, Schendel MJ, Wallace LJ, Ogilvie JW, Gundry CR. Magnetic resonance imaging and biological changes in injured intervertebral discs under normal and increased mechanical demands. *Spine* 1996; 21: 1945-1951, doi: 10.1097/00007632-199609010-00001.
27. Carragee EJ, Don AS, Hurwitz EL, Cuellar JM, Carrino JA, Herzog R. 2009 ISSLS Prize Winner: Does discography cause accelerated progression of degeneration changes in the lumbar disc: a ten-year matched cohort study. *Spine* 2009; 34: 2338-2345, doi: 10.1097/BRS.0b013e3181ab5432.
28. Butler WF. Comparative anatomy and development of the mammalian disc. In: Ghosh P (Editor), *The biology of the intervertebral disc*. Boca Raton: CRC Press; 1989. p 108.
29. Kang JD. Does a needle puncture into the annulus fibrosus cause disc degeneration? *Spine J* 2010; 10: 1106-1107, doi: 10.1016/j.spinee.2010.10.014.
30. Nassr A, Lee JY, Bashir RS, Rihn JA, Eck JC, Kang JD, et al. Does incorrect level needle localization during anterior cervical discectomy and fusion lead to accelerated disc degeneration? *Spine* 2009; 34: 189-192, doi: 10.1097/BRS.0b013e3181913872.
31. Issy-Pereira AC, Castania V, de Jong JJA, Defino HLA, Pitol DL, Iyomasa MM, et al. Modelo de degeneração do disco intervertebral por punção da cauda de ratos Wistar: avaliação histológica e radiográfica. *Coluna/Columna* 2010; 9: 455-461, doi: 10.1590/S1808-18512010000400020.